Figure S1. TAM patterning is affected by host immunocompetence state, related to Figures 2 and 3.

(A) IF image shows UnaG and GLUT1 (glucose transporter 1) expression in pseudopalisading structures of GL261 GBM.

Quantification below: n=20 randomly selected tumor areas from 4 mice per group, unpaired t-test; ***P <0.001. Arrows point to GLUT1$^+$ stromal cells (UnaG$^-$) in hypoxic cores.

(B) Top left, experimental scheme of injection of pimonidazole (Pimo) 1.5 hours before collection of GL261 tumor. Right, fluorescent images show spatial localization of UnaG$^+$ cells in relation to Pimo-labeled cells. Enlarged images of boxed areas are shown below. Arrow in box 3 marks entrapped cells labeled by Pimo but not by UnaG in hypoxic core.

(C) IF images show temporospatial patterns of UnaG$^+$ GBM cells in relation to CD68$^+$ TAMs and tumor vasculature (PECAM1$^+$) during GL261 progression in B6-SCID mice. Arrowhead marks small clusters of UnaG$^+$ GBM cells at 4 wk.

(D) Left, schematic of RCAS GBM induction. Avian RCAS viruses expressing PDGF-B and shRNA against *Trp53* were intracranially injected into C57BL/6 mice carrying Ntva transgene (*Nestin* promoter driving the expression of tv-a virus receptor). Right, IF images and profile plots of immunosignals of marker genes within regions of interest (ROI, dashed brackets) in RCAS GBM. Asterisks denote hypoxic zones. Green lines for GLUT1 and red lines for immune cell markers.

(E) Left, schematic of murine orthotopic CT2A GBM transplant model in syngenetic C57BL/6 host. Right, IF images and profile plots of immunosignals within ROI (dashed brackets) in CT2A GBM. Asterisks denote hypoxic zones. Green lines for GLUT1 and red lines for immune cell markers.

(F) Additional examples of IHC of human GBM samples (tumor microarray GL803c, US Biomax) show spatial patterns of hypoxic areas (GLUT1$^+$) and CD68$^+$ TAMs. Patient ID in the microarray is denoted in each image.
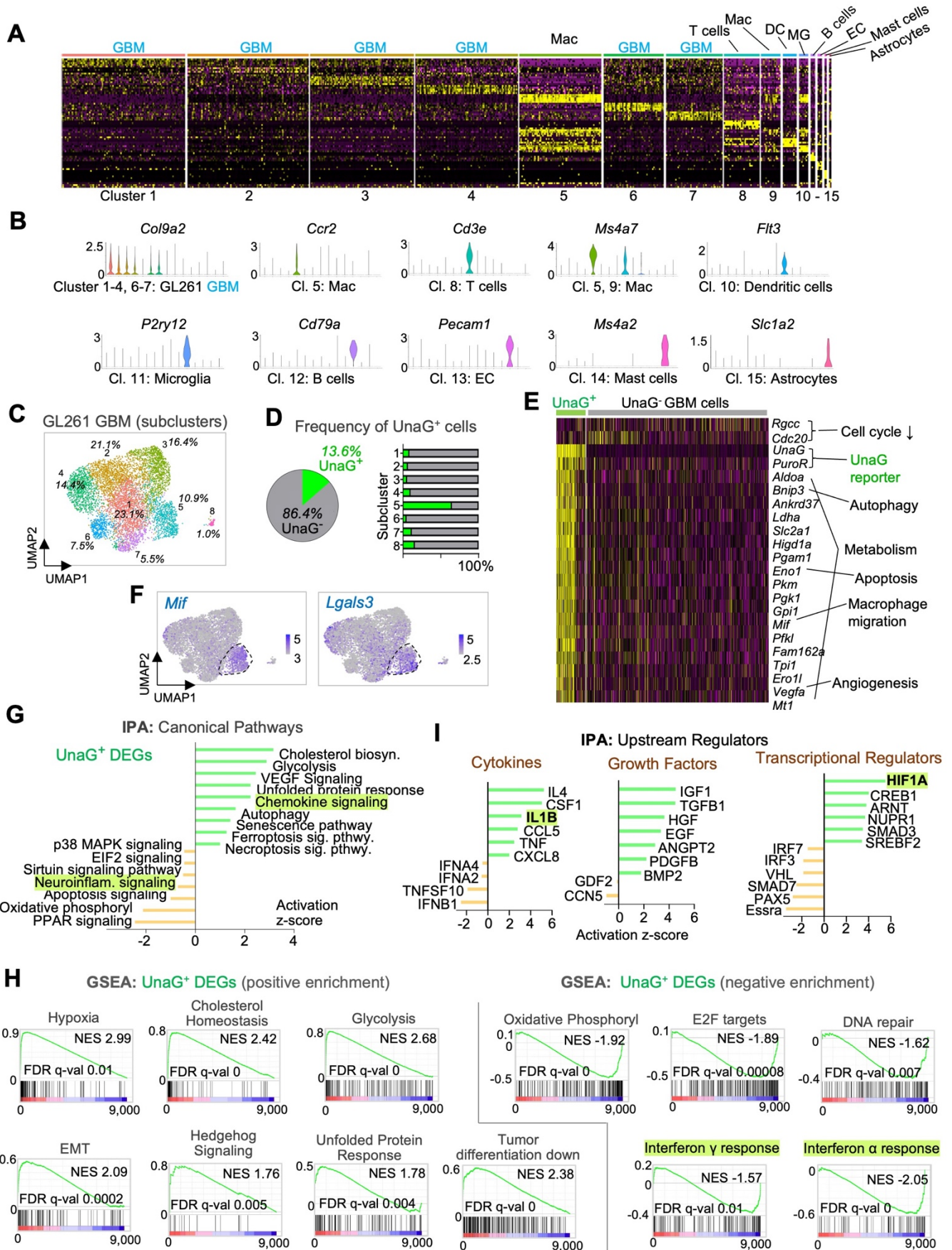
Figure S2. In vivo gene signatures of HIF^ON GBM cells feature immune signaling, related to Figure 5.

(A) Heatmap shows top DEGs in all 15 cell clusters in GL261 tumor.

(B) Violin plots show expression profiles of cell type-specific markers across 15 cell clusters in GL261 tumor.

(C) UMAP plot shows 8 subclusters of GBM cells in GL261 GBM at 4 weeks post-transplant.

(D) Left, pie chart shows the proportion of GBM cells with high or low *UnaG* mRNA reads in GL261 tumor. Right, bar graphs show the proportion of UnaG$^+$ cells among the 8 subclusters of GBM cells.

(E) Heatmap shows top DEGs in UnaG$^+$ vs. UnaG$^-$ GBM cells. Annotation of main functions of the DEGs are shown on the right.

(F) UMAP feature plots show the expression of immune modulatory genes *Mif* and *Lgals3* in GBM cells, with subcluster 5 (UnaG$^+$) outlined by dashed line.

(G) Ingenuity pathway analysis (IPA) of DEGs in UnaG$^+$ vs. UnaG$^-$ GBM cells (cut-off: log$_2$FC ($\pm$) 0.25). Immune pathways are highlighted in green.

(H) Gene set enrichment analysis (GSEA) shows top gene sets with positive or negative enrichment in UnaG$^+$ GBM cells (FDR, false discovery rate; NES, normalized enrichment score). Green highlights negative enrichment for IFNα response and IFNγ response.

(I) IPA prediction of upstream regulators of DEGs in UnaG$^+$ GBM cells, with IL1B and HIF1A highlighted in green.
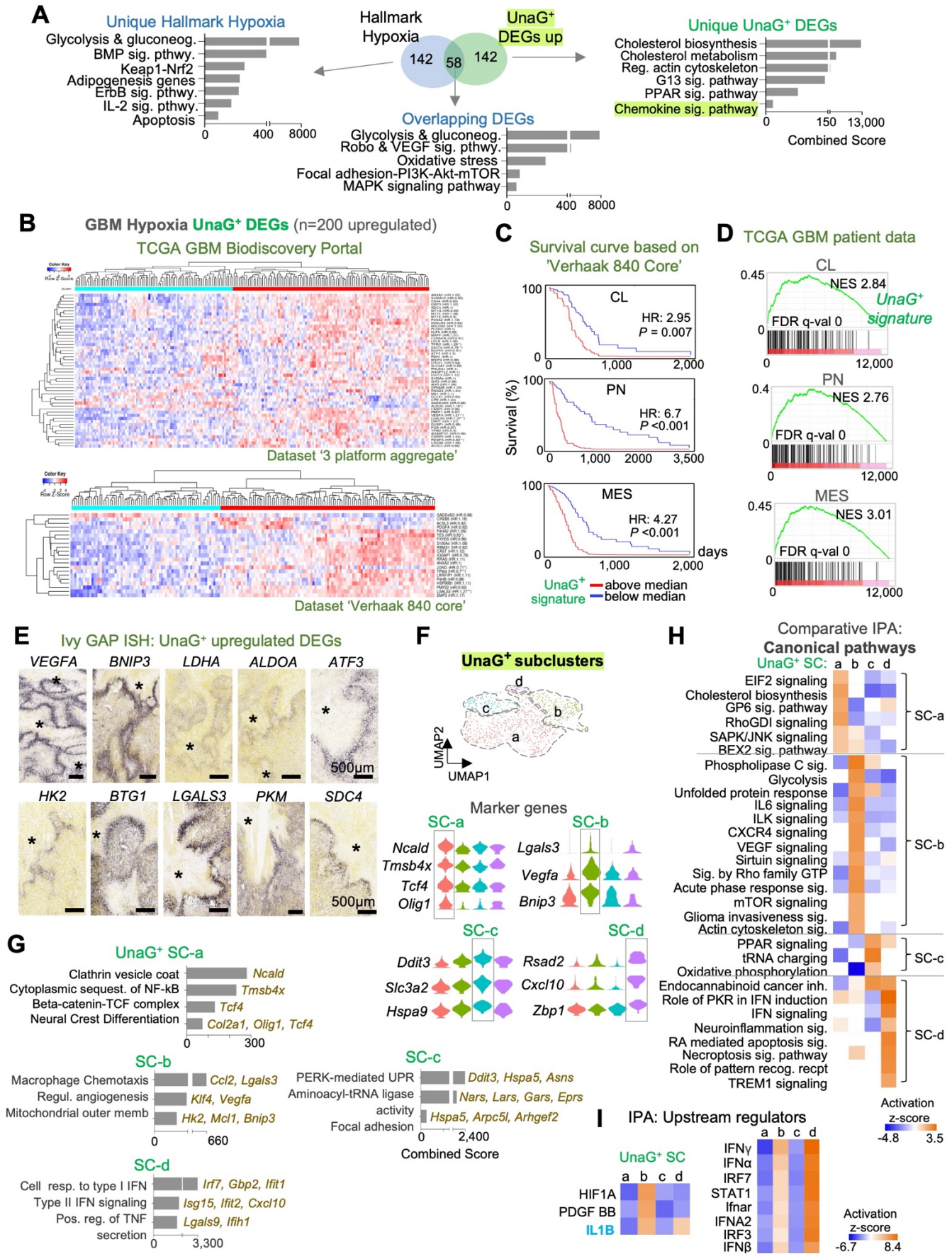
Figure S3. UnaG+ gene signature predicts poor survival for human GBM patients, related to Figure 5.

(A) Center, Venn diagram shows the intersection of UnaG+ DEGs (200 upregulated genes) with "Hallmark Hypoxia" gene

set (MSigDB). Enriched pathways of unique or overlapping genes by Enrichr are shown.

(B) Stratification of human GBM patients according to expression scores for UnaG+ gene signature (top 200 upregulated DEGs in UnaG+ GBM cells). GBM Biodiscovery Portal database: 3 platform aggregates (top) and Verhaak 840 core (bottom).

(C) Kaplan-Meier survival curves of GBM patients stratified into high or low expressors of UnaG+ gene signature. GBM transcriptional subtypes: CL, classical; PN, proneural; MES, mesenchymal. Expression dataset: Verhaak 840 core.

(D) GSEA shows enrichment scores for UnaG+ gene signature (200 upregulated DEGs) in human GBM transcriptional subtypes. For each transcriptional subtype, 12,042 genes from microarray expression data were ranked. NES, normalized enrichment score; FDR, false discovery rate.

(E) In situ mRNA hybridization images from Ivy GAP database show expression patterns of 10 genes from the UnaG+ signature in pseudopalisading structures. Asterisks denote hypoxic cores.

(F) Top, UMAP plot of GL261 scRNA-seq data shows partitioning of UnaG+ GBM cells into four subclusters (SC-a to SC-d). Bottom, violin plots show marker gene expression in each of the four subclusters.

(G) Enrichr analyses (WikiPathways) of enriched pathways in each UnaG+ subcluster.

(H) Comparative IPA show distinct signaling pathways engaged in different subclusters of UnaG+ GBM cells.

(I) Comparative IPA of predicted upstream regulators of DEGs in UnaG+ subclusters, with IL1B highlighted in blue.

A Enrichr, WikiPathways **TAM "yellow" module**

Canonical NFκB ptwy.
IL18 sig. ptwy.
IL1 and megakaryocytes in obesity
Sig. transd. through IL1R
Mods. of TCR sig. and T cell activation
Oxidative damage
HIF1A and PPARγ reg. of glycolysis
IL4 sig. ptwy.
IL1 sig. ptwy.

350 1100
Combined score

B TAM "yellow" module, top DEGs

Gna13 Malt1 Tgm2
Nfil3 Cd14 Cdkn1a Kdm6b
Tnfaip3 Il1b Ifrd1 Cxcr4
Mxd1 Ccrl2 Pim1 Cd83
Pde4b Raf149 Dusp1 Tlr2
Fosl2 Ets2 Epsb Clic4
Ptgs2 Plaur

C *Neftel et al.,* 28 GBM (1,066 stromal cells)

- Dendritic cell
- Diff.-like
- Endothelial
- Fibroblast
- Granulocyte
- Myeloid
- Oligodendrocyte
- Pericyte
- Prolif. stem-like
- Stem-like
- T cell

Granulocytes DC
Myeloid cells

"yellow" gene module

0.3
0.2
0.1
0
-0.1

D GL261 TAM vs. homeostatic MG

-log$_{10}$(P value)
400
300 Snhg11 Cst3
200 Pcsk1n Ifitm3
     Pcp4 Lgals1
     Meg3 Vim
100 Mbp S100a6
     Camk2n1 Lsp1
     Crybb1 Cytip

-2 -1 0 1 2
log$_2$ FC

E Enrichr: DEGs
(TAM vs. homeostatic MG)

Reg. of NK cell chemotaxis
Macrophage chemotaxis
Reg. of T cell chemotaxis
Chemokine recept. binding
Prostaglandin synth. & reg.
Type II IFNγ signaling

500 2000
Combined Score

F TAM subcluster marker genes

Slamf9 *Ly6c2* *Igf1* *Crybb1* *Ncald* *Ccr7* *Xcr1* *Hist1h2ae*
3 (1) 3 (2) 3 (3) 3 (4) 2 (5) 3 (6) 3 (7) 3 (8)
0 0 0 0 0 0 0 0

TAM subclusters

G Enrichr

TAM sc-1 (Proinflammatory)
Macrophage markers
Chemokine sig. pthwy.
IL3 sig. pthwy.
Type III IFN sig.
Neuroinflammation
50 200

TAM sc-2 (*Ccr2+*)
Type-II IFN signaling
IL18 signaling pthwy.
Platelet-mediated inter. with vascular/circulating cells
LTF danger sig. resp. pthwy.
Toll-like receptor pthwy.
320 1100

TAM sc-3 (Hypoxic /immunotolerant)
Glycolysis & Gluconeogen.
HIF1α & PPARγ reg. of glycolysis
IL10 anti-inflamm. sig. ptwy.
VEGFA-VEGFR2 ptwy.
IL4 ptwy.
75 150

TAM sc-4 (Activated microglia)
TYROBP causal network
Microglia pathogen phagocytosis pthwy.
IL18 pthwy.
TGFβR signaling
IL1 sig. pthwy.
100 400

TAM sc-5 (Proliferative/ metabolic)
Electron Transport Chain
Mitochondria complex I
OXPHOS system
TCA cycle
Serine metab.
Mitochondria complex III assembly
375 750

TAM sc-6 (T cell activating Mac)
IL7 sig. pthwy.
TCR sig. pthwy.
Modulators of TCR sig. & T cell activation
IL2 sig. pthwy.
IL17 sig. pthwy.
0 175 350

TAM sc-7 (Angiogenic)
VEGFA-VEGFR2 pthwy.
Interactome of PRC2
mRNA processing
Mechanoregulation and pathology of YAP/TAZ
NAD biosynth. II
120

TAM sc-8 (Proliferative)
DNA replication
DNA mismatch repair
DNA IR-damage/ cellular response via ATR
Homologous recombination
Nucleotide excision repair
375 750
Combined score

H GSEA Hallmark Hypoxia signature score
3
0.6
0
UMAP2 / UMAP1

I Monocle3 pseudotime score
sc-5
sc-3 sc-4
sc-2
sc-7 sc-6
sc-1
sc-8
16 12 8 4 0

J GSEA: Hypoxic TAM (sc-3) DEGs

Positive enrichment
Glycolysis NES 1.49 FDR q-val 0.04
0.4 / 0
Hypoxia NES 1.85 FDR q-val 0.001
0.5 / 0

Negative enrichment
IFNα response NES -2.22 FDR q-val 0
0 / -0.6
IFNγ response NES -2.02 FDR q-val 0
0 / -0.5

7,000

K IPA: Hypoxic TAM (sc-3) DEGs

Canonical Pathways
HIF1α Signaling
IL10 Signaling
eNOS Signaling
Glycolysis
IL8 Signaling
IL13 Signaling
IL33 Signaling
NO & ROS Production
PD-1, PD-L1 Pthwy.
IL17 Signaling
IL4 Signaling
IL2 Signaling and Production
Th1 Pathway
Immunogenic Cell Death Sig. Pthwy.
Macrophage Classical Sig. Pthwy.
AHR Signaling
Interferon Signaling
Oxidative Phos.
EIF2 Signaling

-5 0 5
Activation z-score

L IPA Upstream regulators for Hypoxic TAM (sc-3) DEGs

Cytokines
IL4
CSF1
TNF
IL6
MIF
IL10
IL1B
IFNγ
CXCL2
TNFSF15
IL27
IFNα2
-2 0 2

Growth Factors
TGFB1
EGF
TGFB2
TGFA
TGFB3
VEGFB
GRN
-2 0 2 4

Transmembrane Receptors
PDCD1
CLEC4A
TREM1
IL10RA
CD83
NRP1
CD40
CD86
CD247
CD14
CD28
NCR1
CD244
IFNAR2
-2 0 2

Activation z-score

Figure S4. GL261 GBM harbors a subpopulation of hypoxic TAMs expressing immunosuppressive gene signatures, related to Figures 5 and 6.

(A) Enrichr analysis (WikiPathways) of top co-expressed genes in WGCNA "yellow" (hypoxic) gene module identified in tumor-associated macrophages in GL261 tumor. IL1 and IL1 receptor pathways are highlighted in blue.

(B) Network visualization of co-expressed genes of WGCNA "yellow" (hypoxic) gene module. The network gene *Il1b* is highlighted by arrow.

(C) Mapping of WGCNA "yellow" gene module onto scRNA-seq data from stromal cells of human GBMs (*Neftel et al., 2019*). Myeloid cells, granulocytes and dendritic cells (DC) are shown in enlarged images.

(D) Volcano plot showing DEGs of GL261 TAMs (microglia and macrophages combined) vs. homeostatic microglia (*Zeisel et al., 2018*).

(E) Pathway enrichment analysis of DEGs in TAM vs. homeostatic microglia by Enrichr.

(F) Violin plots show the expression of selected marker genes across eight TAM subclusters in GL261 GBM.

(G) Enrichr analyses (WikiPathways) show pathway enrichment of DEGs in each TAM subcluster, with selected pathways highlighted in blue.

(H) UMAP plot shows expression scores for the "Hallmark Hypoxia" gene set in TAMs, with sc-3 encircled by dashed line.

(I) Pseudotime trajectory analysis of TAM subclusters predicts a differentiation hierarchy starting from node 1 (sc-2) with lineage branching to more differentiated clusters, including sc-3.

(J) GSEA show top gene sets with positive or negative enrichment in sc-3 TAMs. FDR, false discovery rate; NES, normalized enrichment score.

(K) Ingenuity pathway analyses (IPA) show enrichment canonical pathways in sc-3 TAMs vs. other TAMs.

(L) IPA prediction of upstream regulators of DEGs in sc-3 TAMs, with selected regulators highlighted in bold or green.
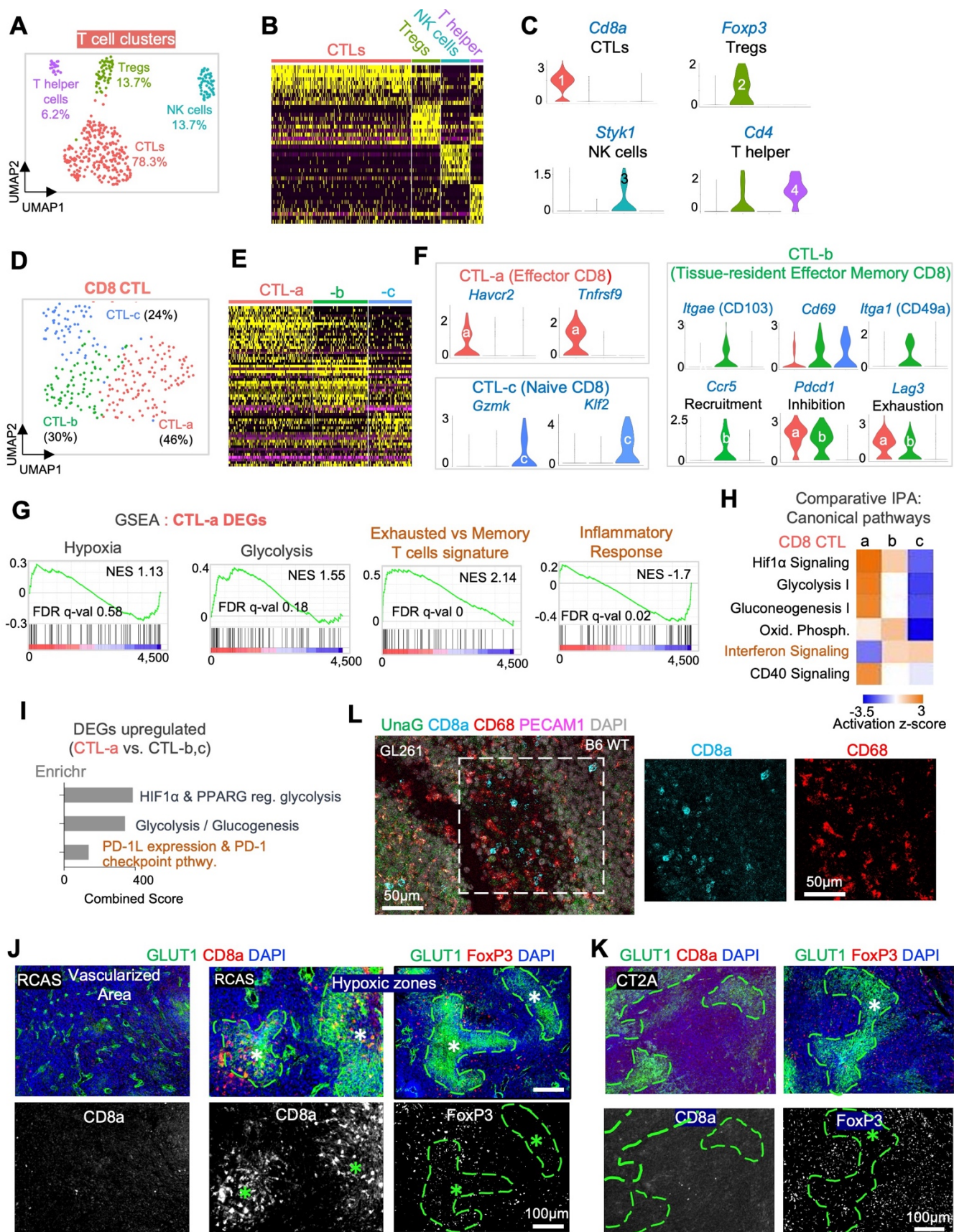
Figure S5. Murine GBM models contain diverse T cell populations with spatial patterning, related to Figure 6.

(A) UMAP shows four T cell subclusters in GL261 GBM.

(B) Heatmap of gene expression in T cell subclusters.

(C) Violin plots show the expression of marker genes used for annotation of T cell subclusters.

(D) UMAP shows three subclusters of CD8 CTL in GL261 GBM.

(E) Heatmap of gene expression in CTL subclusters.

(F) Violin plots show the expression of marker genes that define CTL subclusters, including T cell exhaustion marker *Havcr2,* and *Ccr5*, a canonical receptor for ligand Ccl8, a top DEGs of hypoxic TAMs.

(G) GSEA show positively or negatively enriched gene sets in CTL-a subcluster, with immune gene sets labeled in brown.

(H) Comparative IPA of canonical pathways in CTL subclusters.

(I) Enrichr analysis shows enriched pathways in the 276 upregulated DEGs of subcluster CTL-a.

(J, K) IF images of RCAS (4 weeks post-induction) (J) and CT2A GBM (3 weeks post-transplant) (K) show spatial patterns of CD8a$^+$ CTLs and FOXP3$^+$ Tregs in hypoxic zones outlined by GLUT1 (asterisks) or vascularized areas. The content of CD8a$^+$ CTLs in CT2A GBM at 3 weeks post-transplant was low.

(L) Multiplex 5-color IF image of GL261 GBM shows spatial patterns of CTLs (CD8a) and TAMs (CD68) in relation to hypoxic zones (UnaG) and blood vessels (PECAM1).
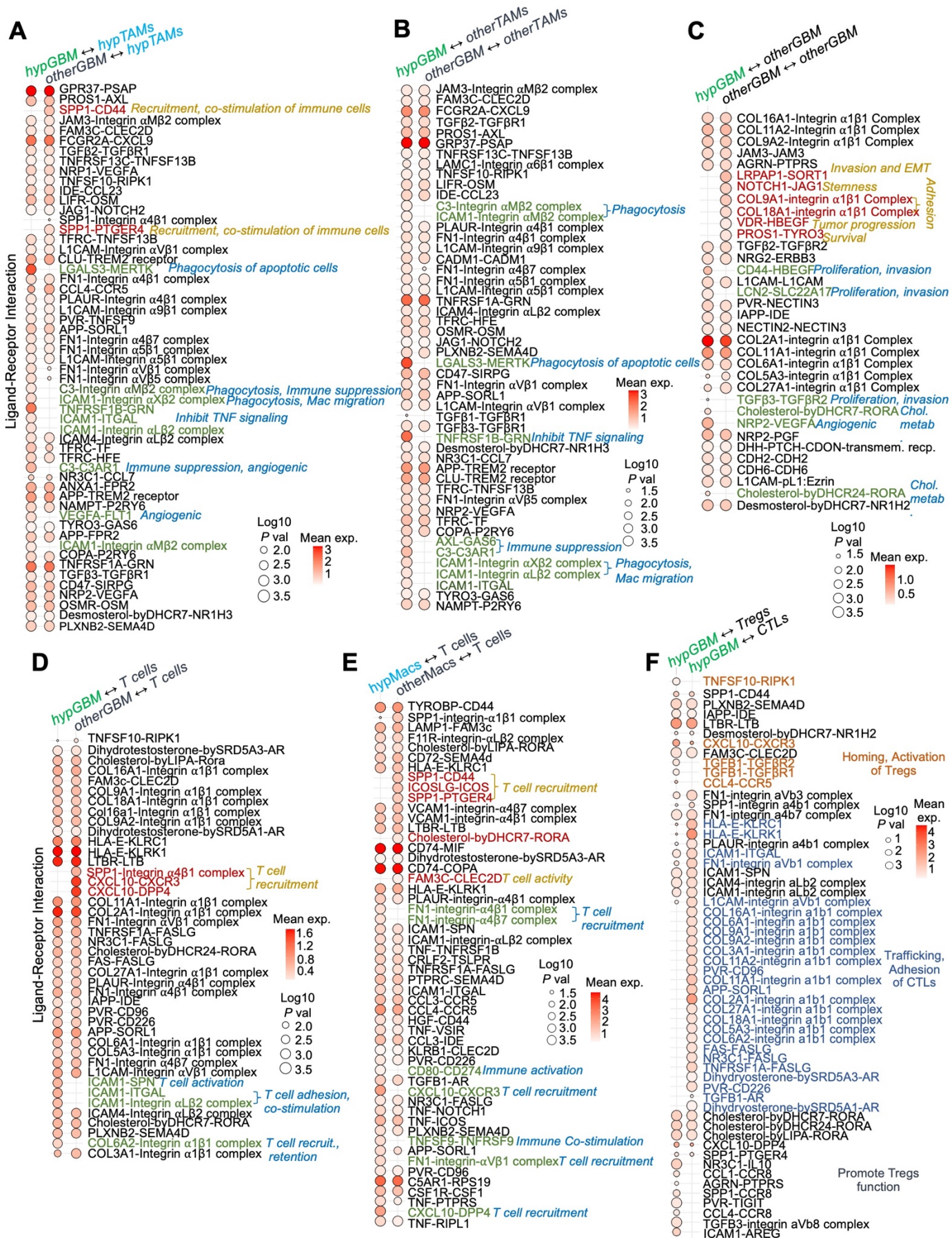
Figure S6. GBM cells and immune cells use distinct signaling communication in hypoxic niches, related to Figure 6.

(A, B) Expression levels of ligand-receptor signaling pairs between GBM cells and TAMs, comparing hypoxic and normoxic (other) GBM cells in their interactions with hypoxic TAMs (A) or normoxic (other) TAMs (B).

(C) Comparison of expression of ligand-receptor signaling pairs between hypoxic or normoxic GBM cells and normoxic GBM cells.

(D) Comparison of expression of ligand-receptor signaling pairs between hypoxic or normoxic GBM cells and T cells.

(E) Comparison of expression of ligand-receptor signaling pairs between hypoxic or normoxic macrophages and T cells.

(F) Comparison of expression of ligand-receptor signaling pairs between hypoxic GBM cells and Tregs or CTLs.
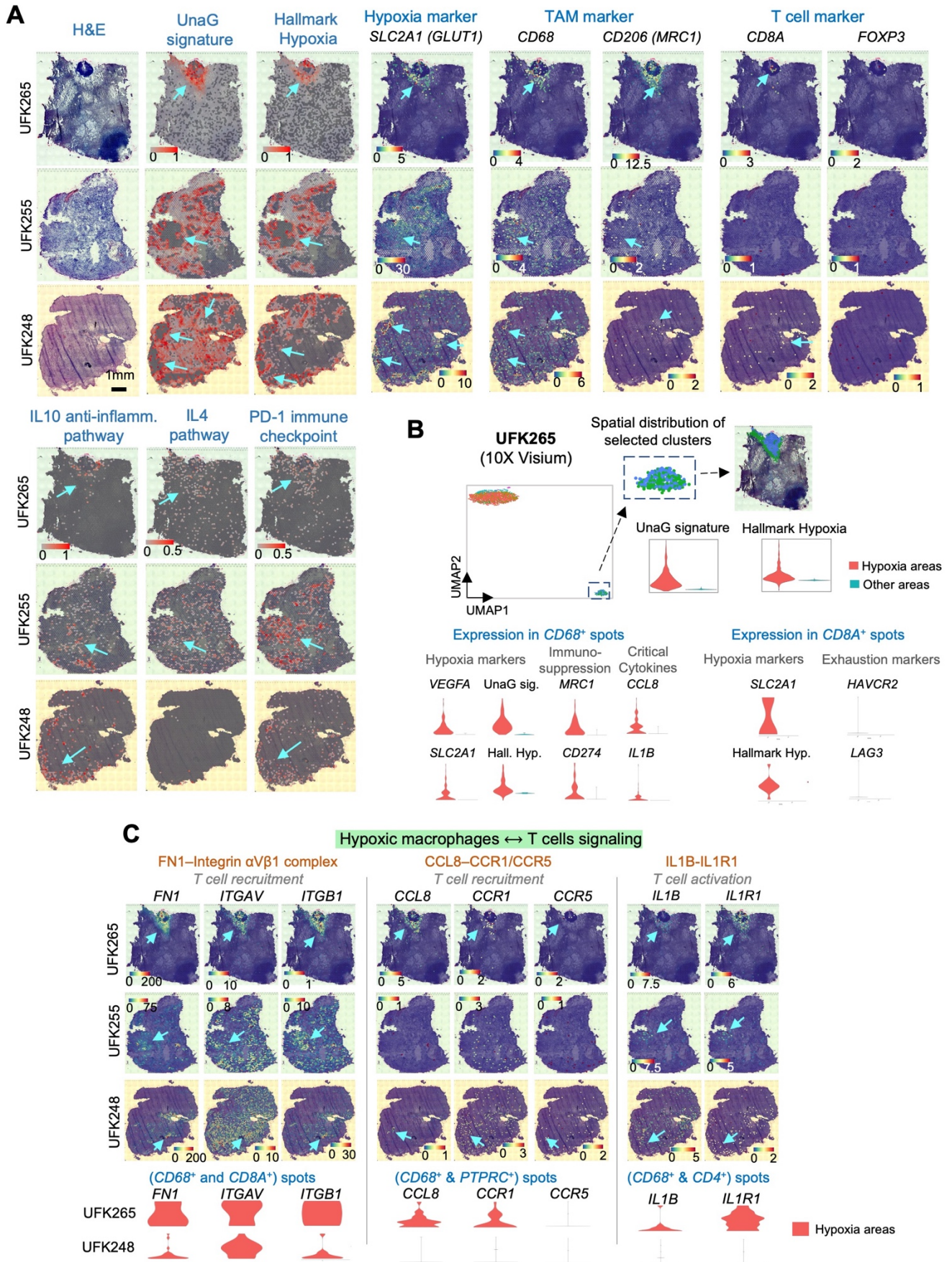
Figure S7. Human GBM spatial transcriptomics reveal hypoxic zones and associated immune cells with hypoxia/immunotolerance gene signatures, related to Figures 6 and 7.

(A) Spatial transcriptomics (10X Visium) of three human GBM specimens show tissue structure (H&E staining) and tissue

spots expressing UnaG signature, "Hallmark Hypoxia" gene set (MSigDB), or the indicated markers. Arrows point to hypoxic zones in pseudopalisading patterns. FOXP3^{+} Tregs were largely absent in hypoxic areas in all three GBM specimens.

(B) Top, UMAP of sequenced spots of human GBM specimen UFK265. Spots (blue & green) displaying high expression scores for UnaG and Hallmark Hypoxia signature genes (shown in violin plots) are marked by dashed box. Spatial localization of these spots (blue & green) in tissue section is shown on top right. Bottom, violin plots show relative expression of marker genes or hypoxic niche chemokine/cytokines (*CCL8* and *IL1B*) in spots positive for TAM marker *CD68* or CTL marker *CD8A* in hypoxic areas vs. other areas.

(C) Top, spatial expression patterns of ligand-receptor pairs in human GBM samples. Arrows point to co-localization of ligand-receptor expression (identified in Fig. S6) in hypoxic zones. UFK265 contained a defined hypoxic zone, whereas UFK248 harbored hypoxic areas in pseudopalisading pattern. FN1-Integrin αVβ1 complex was inferred by CellPhoneDB as signaling between hypoxic TAMs and T cells, while CCL8-CCR1, CCL8-CCR5, and IL1B-IL1R1 signaling pairs were identified by our scRNA-seq. Bottom, violin plots show relative expression of ligand-receptor pairs in spots positive for *CD68* and various T cell markers (*CD8A*, cytotoxic T cells; *PTPRC,* memory T cells; *CD4,* T helper cells) in hypoxic areas vs. other areas.

DATA S1
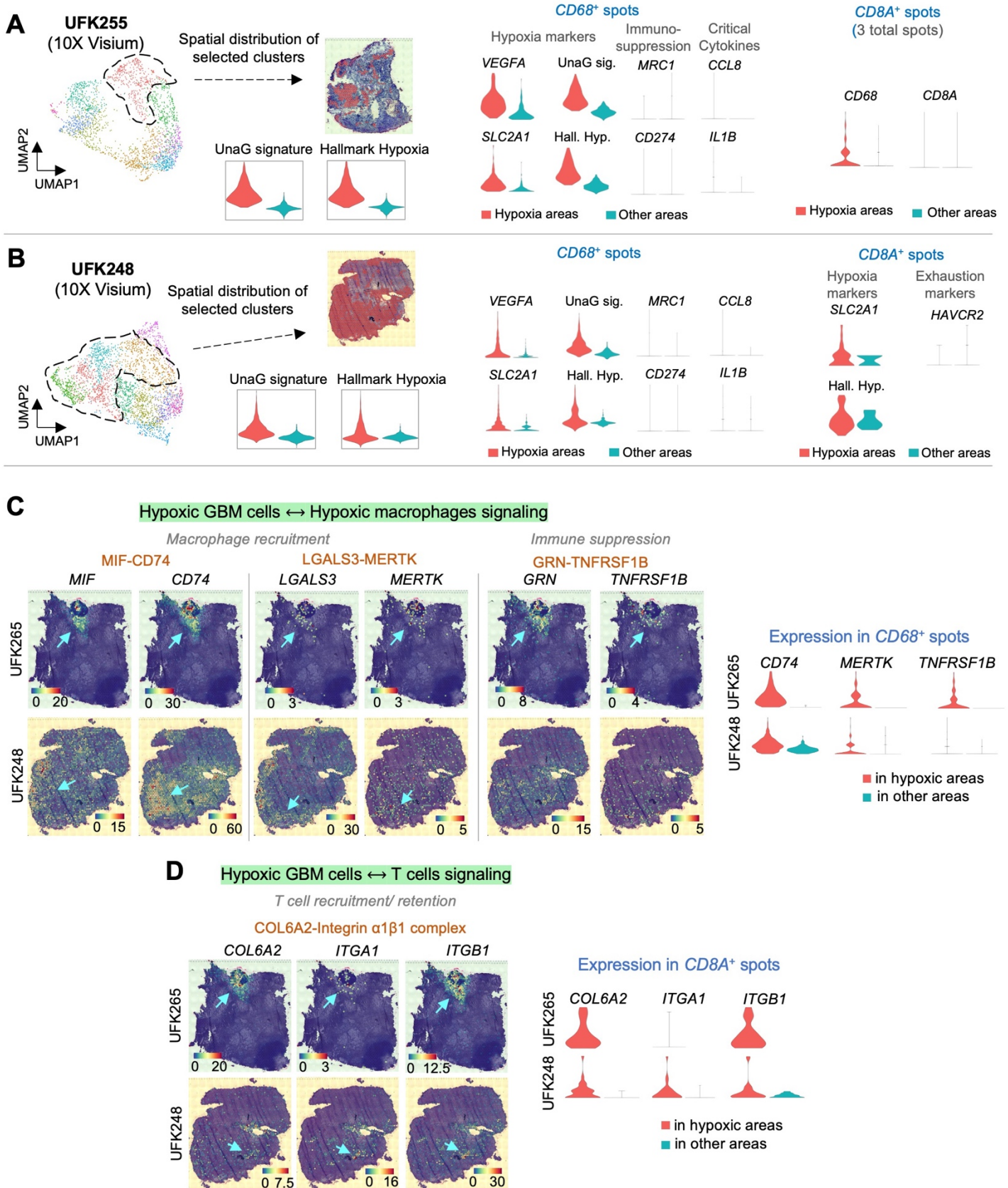
Human GBM spatial transcriptomics confirms patterning of immune cells in hypoxic niches, related to Figure 6, Figure S2 and Figure S6.

(A, B) UMAP of sequenced spots of human GBM specimen UFK255 and UFK248 (10X Visium). Clusters displaying high

expression scores for UnaG and Hallmark Hypoxia signature genes are encircled by dashed lines. Violin plots show gene expression of hypoxia markers or immune genes in spots positive for TAM marker *CD68* or CTL marker *CD8A* in hypoxic areas vs. other areas. UFK255 contains few spots with *CD8A* expression, which expressed *CD68*.

(C) Left, spatial transcriptomics of human GBM (UFK265 and UFK468) show spatial localization of ligand-receptor expression in hypoxic zones (blue arrows). The ligand-receptor pairs were inferred by CellPhoneDB as signaling between hypoxic GBM cells and hypoxic TAMs for macrophage recruitment and immune suppression. *MIF* and *LGALS3* are top DEGs expressed in UnaG⁺ GBM cells (see Fig. S2F). Right, violin plots show relative expression of receptor genes in spots positive for *CD68* expression in hypoxic areas vs. other areas.

(D) Left, spatial localization of spots expressing COL6A2-Integrin α1β1 complex in hypoxic areas of human GBM. This ligand-receptor pair was predicted by CellPhoneDB as signaling between hypoxic GBM cells and T cells for T cell recruitment and retention. Right, violin plots show expression of the ligand-receptor genes in spots with *CD8A* expression in hypoxic areas vs. other areas.
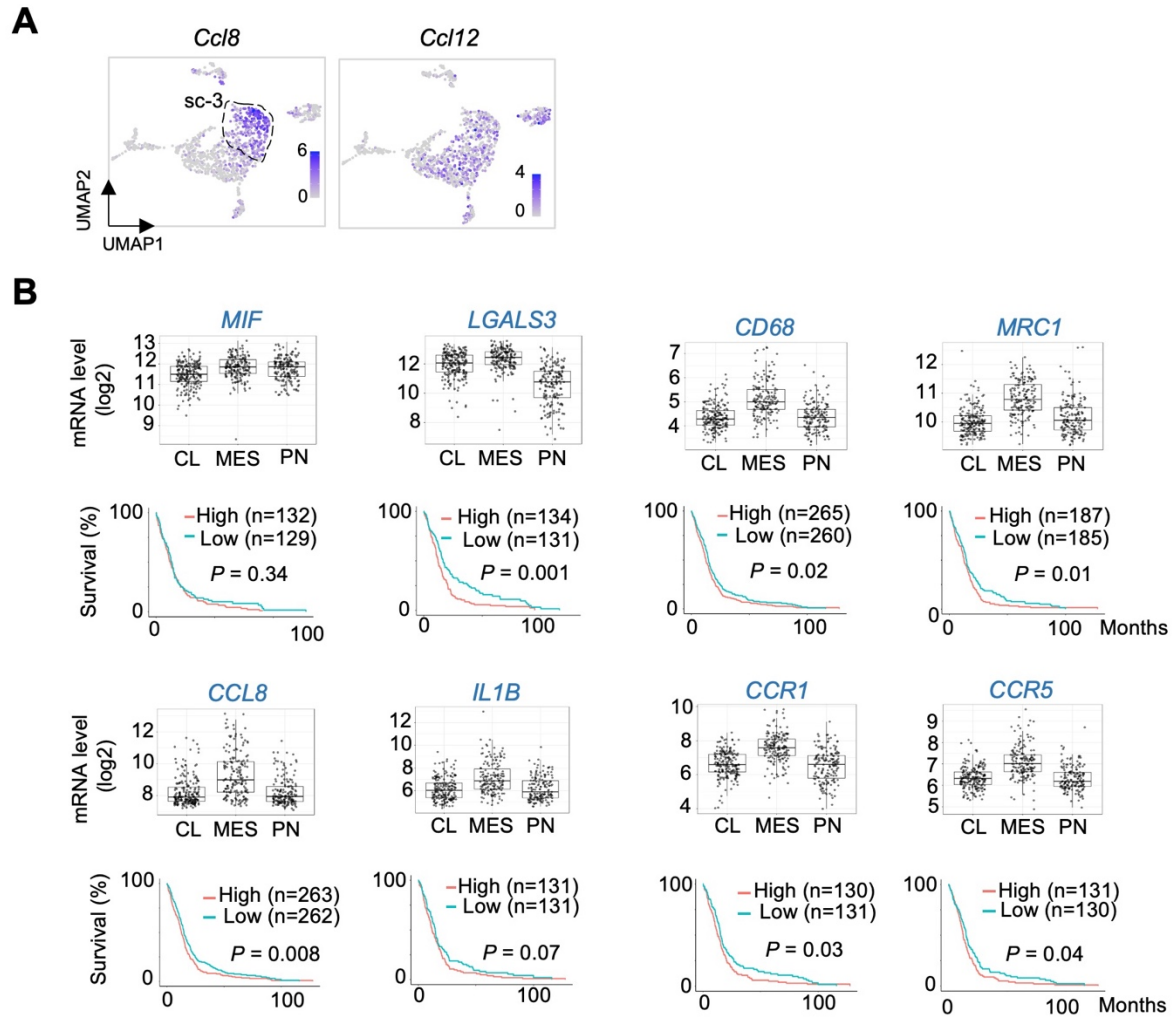
Expression of hypoxic niche genes is associated with GBM malignancy, related to Figure 7.

(A) UMAP feature plots showing the expression of cytokines *Ccl8* and *Ccl12* in TAMs from GL261 tumor. Hypoxic TAMs (sc-3) are encircled by dashed line.

(B) Top rows, box plots of expression of hypoxia-associated cytokines or immune markers in human GBM of different transcriptional subtypes (CL, classical; MES, mesenchymal; PN, proneural). Bottom rows, Kaplan-Meier survival curves of patients stratified into high or low expressors based on median expression of the indicated genes. Graphs generated with Gliovis platform (http://gliovis.bioinfo.cnio.es/).